

TreeNet: A Light Weight Model for Low Bitrate Image Compression

Mahadev Prasad Panda[†], Purnachandra Rao Makkena[†], Srivatsa Prativadibhayankaram^{†§}, Siegfried Fößel[†], André Kaup[§]

[†] *Moving Picture Technologies, Fraunhofer Institute for Integrated Circuits IIS, Erlangen*

[§] *Multimedia Communications and Signal Processing, Friedrich-Alexander-Universität Erlangen-Nürnberg, Erlangen Germany*

Abstract—Reducing computational complexity remains a critical challenge for the widespread adoption of learning-based image compression techniques. In this work, we propose TreeNet, a novel low-complexity image compression model that leverages a binary tree-structured encoder-decoder architecture to achieve efficient representation and reconstruction. We employ attentional feature fusion mechanism to effectively integrate features from multiple branches. We evaluate TreeNet on three widely used benchmark datasets and compare its performance against competing methods including JPEG AI, a recent standard in learning-based image compression. At low bitrates, TreeNet achieves an average improvement of 4.83% in Bjøntegaard delta bitrate over JPEG AI, while reducing model complexity by 87.82%. Furthermore, we conduct extensive ablation studies to investigate the influence of various latent representations within TreeNet, offering deeper insights into the factors contributing to reconstruction.

I. INTRODUCTION

With the proliferation of digital media, lossy image compression becomes vital. Traditional image compression methods such as JPEG2000 [1], BPG [2], and VTM [3] have achieved impressive rate-distortion performance. However, these methods are constrained by their pronounced reliance on complex manually-engineered modules. Recently, end to end optimized learned image compression has gained popularity. The foundational learned compression methods [4], [5] broadly follow the structure of a variational auto-encoder [15]. The analysis transform g_a transforms an image x into a latent representation y . A quantizer \mathcal{Q} quantizes y into a discrete valued latent representation \hat{y} followed by lossless entropy coding using an entropy model $\mathcal{E}_{\hat{y}}$. The synthesis transform g_s maps the entropy decoded latent representation \hat{y}_e to the image space to produce the reconstructed image \hat{x} . The overall process can be summarized as follows:

$$y = g_a(x; \theta), \hat{y} = \mathcal{Q}(y), \hat{y}_e = \mathcal{E}_{\hat{y}}(\hat{y}), \hat{x} = g_s(\hat{y}_e; \phi) \quad (1)$$

where, θ and ϕ represent learnable parameters of g_a and g_s , respectively. As quantization is non-differentiable, uniform noise is added during training to simulate the quantization process [4]. For optimization of such methods the following loss function is used

$$\mathcal{L} = \mathcal{R}(\hat{y}) + \lambda \cdot \mathcal{D}(x, \hat{x}), \quad (2)$$

where $\mathcal{R}(\hat{y})$ represents the bitrate of the discrete latent \hat{y} , and $\mathcal{D}(x, \hat{x})$ indicates the distortion between the original image x

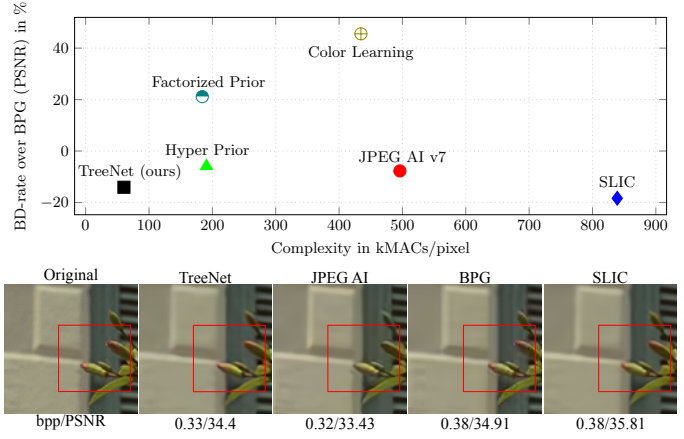


Fig. 1: **Top:** BD-rate for PSNR on Tecnick dataset [17]. TreeNet achieves better trade-off between coding performance and complexity. **Bottom:** Comparison of decoded patches on *kodim06* image from Kodak dataset [18].

and the reconstructed image \hat{x} . The Lagrangian multiplier λ controls the trade-off between rate and distortion.

Several works concentrating on different facets of learned image compression, such as network design [9], [10], context modeling [7], [19], [12], [11], [13], [14] etc. have been proposed to enhance rate-distortion performance. Remarkably, some learned image compression methods [11], [13], [14] are outperforming state-of-the-art traditional methods like the intra-coding mode of VVC. Recently, the JPEG standardization committee has introduced JPEG AI [16], a learning-based image coding standard. However, to achieve better rate-distortion performance, these methods often necessitate complex model architectures, which limits their widespread adoption. Various approaches have been introduced to address the computational cost associated with learned image compression. In [12], [19] faster context models are proposed to accelerate encoding and decoding processes. Transformer-based architectures [20], [21] have also been investigated to enhance computational efficiency, primarily through the parallel processing of independent sub-tensors. Highly asymmetric encoder-decoder architectures where the decoder is significantly less complex than the encoder have been proposed in [22], [23]; though, the overall complexity remains high. Low complexity overfitted neural networks based on implicit

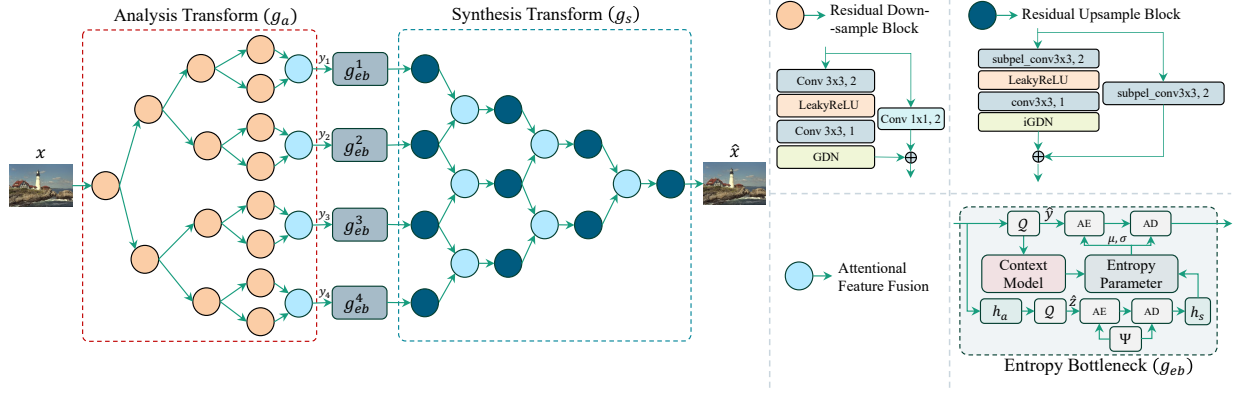


Fig. 2: Schematic diagram for TreeNet. A binary tree-based analysis transform g_a maps image x into four latents y_1, y_2, y_3 , and y_4 . These latents are independently quantized and entropy coded using four entropy bottleneck blocks $g_{eb}^1, g_{eb}^2, g_{eb}^3$, and g_{eb}^4 . The synthesis transform g_s maps latents to image space producing reconstructed image \hat{x} . The attentional feature fusion is as described in [28].

neural representations have also been investigated for image compression [24], [25], [26]. However, the time required for overfitting such networks poses a critical challenge.

In contrast to these approaches, our work focuses on designing a computationally less complex architecture for both the encoder and the decoder. Moreover, the proposed method is amenable to further optimization through parallel processing. With this context, we introduce TreeNet, a learning-based image compression model that takes advantage of a binary tree-structured encoder and decoder architecture. Such tree-structured network has previously been explored for image denoising applications in [27]. Unlike the model proposed in [27], our approach does not involve splitting of tensors. Furthermore, we incorporate attention-based feature fusion [28] modules to combine features from different branches. Concretely, our contributions are summarized as follows,

- We introduce a novel and computationally efficient learned image compression model, TreeNet, featuring a tree-based encoder and decoder design.
- We provide a thorough evaluation of TreeNet, including both qualitative and quantitative performance analyses, as well as a detailed assessment of the model complexity.
- Through extensive experimentation, we elucidate the influence of various latent representations in TreeNet on the reconstructed image, thereby making our model more interpretable.

II. MODEL ARCHITECTURE

In this section, we describe TreeNet in detail. Fig. 2 illustrates the schematic representation of the model architecture. The model consists of an analysis transform $g_a(\cdot)$, four entropy bottlenecks $g_{eb}(\cdot)$, and a synthesis transform $g_s(\cdot)$. The analysis transform g_a is designed as a perfect binary tree with a height of 3 encompassing 8 leaf nodes, each functioning as a learnable block. In our experiments, the nodes in g_a are structured as residual downsampling blocks as depicted in Fig. 2. The input image x is processed by the root node of g_a . The preceding nodes form the input to the successive nodes, i.e., the two child nodes of each parent node receive identical

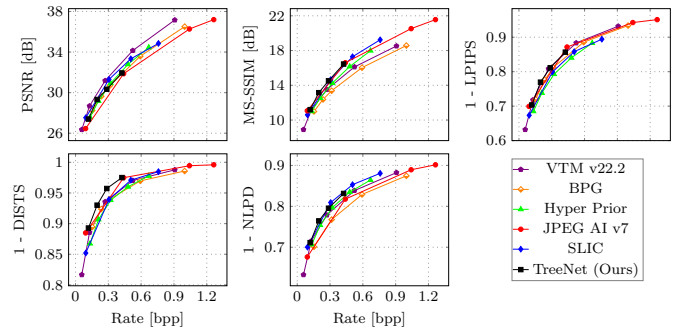


Fig. 3: RD curves on Kodak dataset [18].

input feature maps. This is done so that during training, the two child nodes have the scope of capturing unique and complimentary features from the complete input. We combine the feature maps emerging from the leaf nodes with common parent nodes using attentional feature fusion [28]. This results in four latents y_1, y_2, y_3 , and y_4 which are then sent to four different entropy bottlenecks for latent specific entropy coding.

The architecture of each entropy bottleneck is same as in [10] consisting of a hyper analysis transform $h_a(\cdot)$, a context model $g_c(\cdot)$, a hyper synthesis transform $h_s(\cdot)$, and an entropy parameter estimation block $h_{ep}(\cdot)$. However, instead of an autoregressive context model, we utilize the checkerboard context model [12] for faster inference.

The output of four entropy bottlenecks is fed into the synthesis transform g_s . The synthesis transform consists of three upsampling layers. Each upsampling layer contains N residual upsample nodes and $N-1$ feature fusion nodes, where $N \in \{3, 2, 1\}$. In each feature fusion node, the outputs from two residual upsample nodes are combined, as illustrated in Fig. 2. In the end, a single residual upsample node generates the reconstructed image \hat{x} utilizing the features received from the preceding upsampling layer. Existing model architectures [6], [7], [10], [11] use 128 or 192 channels in the convolutional layers. However, TreeNet is configured with 32 channels, which reduces the complexity further.

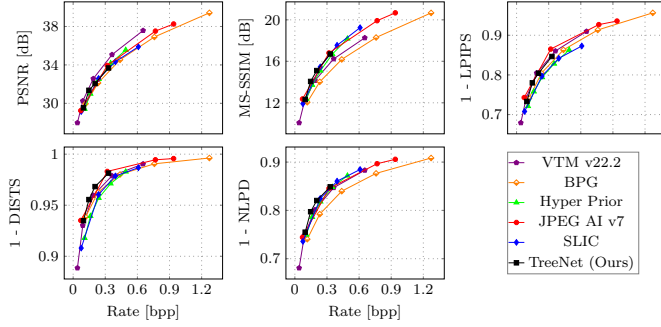


Fig. 4: RD curves on CLIC Professional Valid dataset [31].

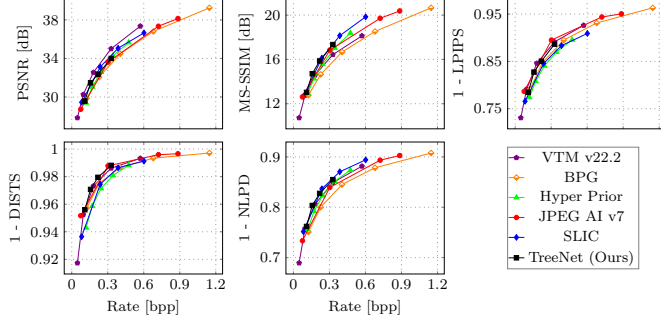


Fig. 5: RD curves on Tecnick dataset [17].

III. EXPERIMENTS

A. Training Setup

We trained the models on the combined train and test set of COCO 2017 dataset [29] consisting 150,000 images. We randomly cropped patches of size 256×256 from the original images for training. The models are trained with a batch size of 16 with random shuffling. For training the models following loss function was utilized,

$$\begin{aligned}
 \mathcal{L} &= \mathcal{R}(\hat{y}, \hat{z}) + \lambda \cdot \mathcal{D}(x, \hat{x}) \\
 &= \mathbb{E}_{x \sim p_x} \left[- \sum_{i=0}^3 \left(\log_2(\mathcal{E}_{(\hat{y}_i | \hat{z}_i)}^i(\hat{y}_i | \hat{z}_i)) + \log_2(\mathcal{E}_{(\hat{z}_i | \Psi)}^i(\hat{z}_i | \Psi)) \right) \right] \\
 &+ \lambda_1 \cdot \mathbb{E}_{x \sim p_x} [MSE(x, \hat{x})] \\
 &+ \lambda_2 \cdot \mathbb{E}_{x \sim p_x} [1 - MS-SSIM(x, \hat{x})] \\
 \hat{x} &= g_s(g_{eb}(g_a(x))) \tag{4}
 \end{aligned}$$

where, \mathcal{R} represents rate, λ_1 and λ_2 are Lagrangian multipliers, and Ψ indicates factorized prior. We compute the mean square error (MSE) and the multi-scale SSIM ($MS-SSIM$) between the original and reconstructed images as distortion measures. In our experiments, we empirically found λ_1 to be $\{0.01, 0.005, 0.0025, 0.00125\}$ and λ_2 to be $\{2.4, 1.2, 0.6, 0.3\}$ culminating in a bitrate between 0.1 and 0.4 bpp. For optimization we used Adam [30] optimizer with an initial learning rate of 10^{-4} . Each model corresponding to a λ value is trained for 450 epochs.

B. Testing Setup

For evaluation, we used Kodak [18], CLIC Professional Valid [31], and Tecnick [17] datasets. We benchmarked TreeNet against BPG [2], VTM [3], JPEG AI [16], Factorized

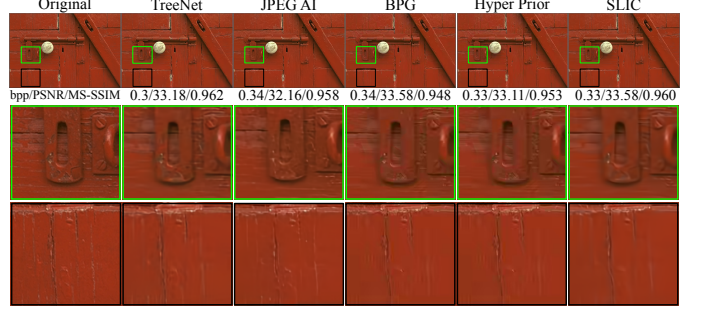


Fig. 6: Visual comparison of reconstructed images and enlarged patches on *kodim02* image from Kodak dataset [18].

Prior [4], Hyper Prior [6], Color Learning [8] and SLIC [9]. For quantitative comparison, we computed quality metrics such as PSNR, MS-SSIM [32], LPIPS [33], and DISTs [34] using PyTorch Image Quality package [35]. Additionally, we compute NLPD [36] using the implementation provided in [37]. We also calculate Bjøntegaard delta bitrate (BD-rate) [38] for comparing different codecs.

IV. RESULTS

A. Quantitative Comparison

For evaluating the performance of TreeNet quantitatively, we compute the rate-distortion (RD) performance on datasets as mentioned in Subsection III-B. The BD-rate computations are reported in Table I and the RD plots are shown in Fig. 3, 4, and 5. Overall, TreeNet outperforms Factorized Prior [4], Color Learning [8], Hyper Prior [6], and BPG [2], while performing competitively compared to VTM [3], JPEG AI [16], and SLIC [9] across all metrics. TreeNet has an average BD-rate gain in PSNR of 4.83% over JPEG AI. Notably, TreeNet has BD-rate savings of 12.50% in NLPD metric over JPEG AI [16] while being significantly less complex.

B. Qualitative Comparison

To showcase the efficacy of TreeNet to produce high quality reconstructions, we visually compare the output of various methods to that of TreeNet as shown in Fig. 6. Along with the overall comparison, we focus on specific areas of the image to highlight the differences. Upon closer inspection, we observe TreeNet has higher reconstruction fidelity both in terms of structure and color compared to other codecs. Even though structural fidelity of JPEG AI [16] is better compared to our method, TreeNet outperforms it in terms of color fidelity. We observe that subtle changes in color are well preserved in TreeNet.

C. Complexity Analysis

For quantifying complexity, we compute thousand multiply-accumulate operations per pixel (kMACs/pixel) using torchinfo¹ module. Table II depicts a comparison of kMACs/pixel of various learning-based models. The overall complexity for TreeNet encompassing both encoder and decoder is 60.4 kMACs/pixel. Out of this, the decoder accounts

¹<https://github.com/TylerYep/torchinfo>

TABLE I: BD-rate (%) comparison. **Red** represents the best performance and **blue** indicates the second best performance.

Methods	Kodak [18]				CLIC Professional Valid [31]				Tecnick [17]			
	PSNR	MS-SSIM	1-NLPD	1-LPIPS	PSNR	MS-SSIM	1-NLPD	1-LPIPS	PSNR	MS-SSIM	1-NLPD	1-LPIPS
BPG [2]	0	0	0	0	0	0	0	0	0	0	0	0
VTM [3]	-22.62	-15.01	-23.52	-10.93	-27.98	-20.20	-27.46	-17.39	-28.93	-16.27	-25.50	-17.65
Color Learning [8]	49.03	-7.02	-6.59	31.60	41.28	-7.63	-3.55	22.10	45.55	1.23	7.26	33.86
Factorized Prior [4]	23.88	-14.59	-15.97	30.22	24.01	-16.77	-11.04	39.42	21.13	-7.33	-1.63	37.71
Hyper Prior [6]	-2.39	-18.80	-23.18	19.84	-7.60	-26.79	-26.07	15.27	-5.88	-19.16	-18.51	15.99
SLIC [9]	-13.67	-30.31	-35.65	9.23	-8.65	-34.05	-31.80	12.81	-18.37	-33.07	-33.46	7.77
JPEG AI [16]	7.47	-37.51	-14.36	2.12	-15.06	-38.61	-33.11	-24.71	-8.30	-29.08	-17.62	-17.09
TreeNet (Ours)	-2.95	-32.15	-33.30	-10.18	-13.34	-35.05	-38.17	-13.72	-14.08	-30.73	-31.31	-10.52

TABLE II: Complexity comparison of various codecs.

Codec Names	Encoder Complexity [kMACs/pixel]	Decoder Complexity [kMACs/pixel]
TreeNet (ours)	9.32	51.08
Factorized Prior	36.84	147.25
Hyper Prior	40.80	149.89
JPEG AI	277.16	218.83
Color Learning	128.89	305.58
SLIC	93.52	745.57

TABLE III: Complexity analysis of TreeNet.

Module Names	Complexity [kMACs/pixel]	No. Params. [millions]
g_a	6.86	0.32
g_s	49.89	0.86
h_a ($\times 4$)	0.37	0.19
h_s ($\times 4$)	0.85	0.68
h_{ep} ($\times 4$)	0.8	0.03
Context Model ($\times 4$)	0.44	0.21

for 51.08 kMACs/pixel, while the encoder contributes 9.32 kMACs/pixel. Notably, TreeNet has 87.82 % less complexity compared to JPEG AI (495.99 kMACs/pixel). We further compute module-wise complexities along with the number of parameters for TreeNet and report them in Table III.

D. Ablation Study

1) *Latent Interpretation*: For showcasing the impact of four input feature maps of g_s on the reconstructed image, we conducted eight experiments belonging to two broad categories, namely, selective propagation and accumulative propagation.

In selective propagation, we provide a single input feature map out of the four to g_s at a time as shown in (5) and inspect the output. In doing so, we determine the influence of each feature map in the pixel space.

$$o_i^{sp} = g_s(y_i); i \in \{1, 2, 3, 4\} \quad (5)$$

The first four columns in Fig. 7, depict the output o_i^{sp} when individual input feature maps are provided to g_s . From these columns we can infer that y_1 and y_2 are responsible for reconstruction of low frequency and high frequency contents in the image, whereas y_3 and y_4 impart color to the reconstruction. Secondly, in accumulative propagation, we gradually accumulate the input to g_s one after the other, starting from the feature map y_1 as shown in (6).

$$\begin{aligned} o_i^{ac} &= g_s(y_i^{ac}); i \in \{1, 2, 3, 4\}; \\ y_i^{ac} &\in \{(y_1), (y_1, y_2), (y_1, y_2, y_3), (y_1, y_2, y_3, y_4)\} \end{aligned} \quad (6)$$

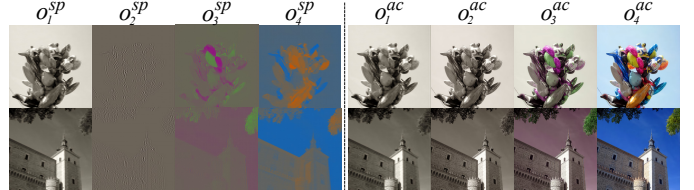


Fig. 7: Visualization of latent interpretation $RGB_OR_1200 \times 1200_014$ and $RGB_OR_1200 \times 1200_005$ images from Tecnick dataset [17].

We showcase the effect of such accumulative propagation in pixel space in the last four columns of Fig. 7. We observe that providing y_1 as input to g_s produces a low frequency output image. Providing y_1 and y_2 together results in the luma component of the image. As we accumulate y_3 and y_4 feature maps in the input, color components get added to the reconstructed image. Note that TreeNet decomposes the features into luma and chroma components without being directly supervised to do so during training.

2) *Spatial Rate Distribution*: We visualize the average number of bits required for encoding the latent feature maps. The bitmap is computed by averaging likelihoods for latent pixels across channels. Formally, the bitmap generation process can be stated as

$$M_{y_i} = \Omega \left(-\frac{1}{C} \sum_{j=0}^{C-1} \log_2 \left(\mathcal{E}_{\hat{y}_{ij} | \hat{z}_{ij}} (\hat{y}_{ij} | \hat{z}_{ij}) \right) \right) \quad (7)$$

where M_{y_i} represents the upscaled bitmap used for visualization. $\Omega(\cdot)$ is the nearest neighbour operation used for scaling the bitmap to image dimension, C is the number of channels in a latent feature map, \hat{y}_{ij} indicates the j^{th} channel of i^{th} quantized latent \hat{y} , and \hat{z}_{ij} represents the j^{th} channel of i^{th} quantized hyper-latent \hat{z} .

We visualize the bitmaps alongside the original image in Fig. 8. For latent y_1 , the bitmap is more spread out compared to that for latent y_2 for which the bitmap is concentrated around the high frequency parts of the image. The bitmaps for latents y_3 and y_4 present the focus on color gradient. The checkerboard patterns that are visible in bitmaps are due to the checkerboard context model.

V. CONCLUSION

In this paper, we propose a novel learning-based image compression method called TreeNet that leverages a binary tree-structured architecture for complexity reduction. We present a

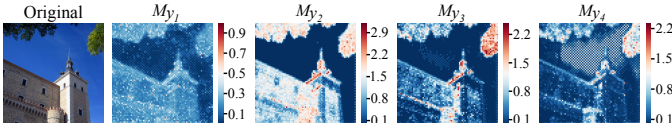


Fig. 8: Bitmaps for $RGB_OR_1200 \times 1200_005$ image from Tecnick dataset [17].

detailed quantitative and qualitative evaluation of our method and compare it with various state-of-the-art methods including JPEG AI. The experiments showcase competitiveness of TreeNet across three test sets in the five evaluation metrics while being significantly less complex. Finally, we elucidate the contribution of latent blocks on reconstruction providing interpretability to our model. In future work, we aim to further reduce the decoder complexity and improve the rate-distortion performance through better context modeling.

REFERENCES

- [1] A. Skodras, C. Christopoulos, and T. Ebrahimi, “The jpeg 2000 still image compression standard,” *IEEE Signal processing magazine*, vol. 18, no. 5, pp. 36–58, 2001.
- [2] G. J. Sullivan, J.-R. Ohm, W.-J. Han, and T. Wiegand, “Overview of the high efficiency video coding (hevc) standard,” *IEEE Transactions on circuits and systems for video technology*, vol. 22, no. 12, pp. 1649–1668, 2012.
- [3] B. Bross, Y.-K. Wang, Y. Ye, S. Liu, J. Chen, G. J. Sullivan, and J.-R. Ohm, “Overview of the versatile video coding (vvc) standard and its applications,” *IEEE Transactions on Circuits and Systems for Video Technology*, vol. 31, no. 10, pp. 3736–3764, 2021.
- [4] J. Ballé, V. Laparra, and E. P. Simoncelli, “End-to-end optimized image compression,” in *International Conference on Learning Representations*, 2017.
- [5] L. Theis, W. Shi, A. Cunningham, and F. Huszár, “Lossy image compression with compressive autoencoders,” in *International Conference on Learning Representations*, 2017.
- [6] J. Ballé, D. Minnen, S. Singh, S. J. Hwang, and N. Johnston, “Variational image compression with a scale hyperprior,” in *International Conference on Learning Representations*, 2018.
- [7] D. Minnen, J. Ballé, and G. D. Toderici, “Joint autoregressive and hierarchical priors for learned image compression,” in *Advances in Neural Information Processing Systems*, S. Bengio, H. Wallach, H. Larochelle, K. Grauman, N. Cesa-Bianchi, and R. Garnett, Eds., vol. 31. Curran Associates, Inc., 2018.
- [8] S. Pratavadihayankaram, T. Richter, H. Sparenberg, and S. Foessel, “Color learning for image compression,” in *2023 IEEE International Conference on Image Processing (ICIP)*. IEEE, 2023, pp. 2330–2334.
- [9] S. Pratavadihayankaram, M. P. Panda, T. Richter, H. Sparenberg, S. Fößel, and A. Kaup, “Slic: a learned image codec using structure and color,” in *2024 Data Compression Conference (DCC)*. IEEE, 2024, pp. 3–12.
- [10] Z. Cheng, H. Sun, M. Takeuchi, and J. Katto, “Learned image compression with discretized gaussian mixture likelihoods and attention modules,” in *Proceedings of the IEEE/CVF conference on computer vision and pattern recognition*, 2020, pp. 7939–7948.
- [11] D. He, Z. Yang, W. Peng, R. Ma, H. Qin, and Y. Wang, “Elic: Efficient learned image compression with unevenly grouped space-channel contextual adaptive coding,” in *Proceedings of the IEEE/CVF Conference on Computer Vision and Pattern Recognition*, 2022, pp. 5718–5727.
- [12] D. He, Y. Zheng, B. Sun, Y. Wang, and H. Qin, “Checkerboard context model for efficient learned image compression,” in *Proceedings of the IEEE/CVF Conference on Computer Vision and Pattern Recognition*, 2021, pp. 14771–14780.
- [13] W. Jiang, J. Yang, Y. Zhai, P. Ning, F. Gao, and R. Wang, “Mlic: Multi-reference entropy model for learned image compression,” in *Proceedings of the 31st ACM International Conference on Multimedia*, 2023, pp. 7618–7627.
- [14] W. Jiang, J. Yang, Y. Zhai, F. Gao, and R. Wang, “Mlic++: Linear complexity multi-reference entropy modeling for learned image compression,” *arXiv preprint arXiv:2307.15421*, 2023.
- [15] D. P. Kingma, M. Welling *et al.*, “Auto-encoding variational bayes,” 2013.
- [16] E. Alshina, J. Ascenso, and T. Ebrahimi, “Jpeg ai: The first international standard for image coding based on an end-to-end learning-based approach,” *IEEE MultiMedia*, vol. 31, no. 4, pp. 60–69, 2024.
- [17] N. Asuni, A. Giachetti *et al.*, “Testimages: a large-scale archive for testing visual devices and basic image processing algorithms.” in *STAG*, 2014, pp. 63–70.
- [18] E. Kodak, “Kodak lossless true color image suite,” *Tech. Rep.*, 1993.
- [19] D. Minnen and S. Singh, “Channel-wise autoregressive entropy models for learned image compression,” in *2020 IEEE International Conference on Image Processing (ICIP)*. IEEE, 2020, pp. 3339–3343.
- [20] F. Mentzer, E. Agustsson, and M. Tschannen, “M2t: Masking transformers twice for faster decoding,” in *Proceedings of the IEEE/CVF International Conference on Computer Vision*, 2023, pp. 5340–5349.
- [21] Y. Zhu, Y. Yang, and T. Cohen, “Transformer-based transform coding,” in *International Conference on Learning Representations*, 2022.
- [22] Y. Yang and S. Mandt, “Computationally-efficient neural image compression with shallow decoders,” in *Proceedings of the IEEE/CVF International Conference on Computer Vision*, 2023, pp. 530–540.
- [23] F. Galpin, M. Balcilar, F. Lefebvre, F. Racapé, and P. Hellier, “Entropy coding improvement for low-complexity compressive auto-encoders,” in *2023 Data Compression Conference (DCC)*, 2023, pp. 338–338.
- [24] T. Leguay, T. Ladune, P. Philippe, G. Clare, F. Henry, and O. Déforges, “Low-complexity overfitted neural image codec,” in *2023 IEEE 25th International Workshop on Multimedia Signal Processing (MMSP)*. IEEE, 2023, pp. 1–6.
- [25] H. Kim, M. Bauer, L. Theis, J. R. Schwarz, and E. Dupont, “C3: High-performance and low-complexity neural compression from a single image or video,” in *Proceedings of the IEEE/CVF Conference on Computer Vision and Pattern Recognition*, 2024, pp. 9347–9358.
- [26] T. Blard, T. Ladune, P. Philippe, G. Clare, X. Jiang, and O. Déforges, “Overfitted image coding at reduced complexity,” in *2024 32nd European Signal Processing Conference (EUSIPCO)*. IEEE, 2024, pp. 927–931.
- [27] R. Flepp, A. Ignatov, R. Timofte, and L. Van Gool, “Real-world mobile image denoising dataset with efficient baselines,” in *Proceedings of the IEEE/CVF Conference on Computer Vision and Pattern Recognition*, 2024, pp. 22368–22377.
- [28] Y. Dai, F. Gieseke, S. Oehmcke, Y. Wu, and K. Barnard, “Attentional feature fusion,” in *IEEE Winter Conference on Applications of Computer Vision, WACV 2021*, 2021.
- [29] T.-Y. Lin, M. Maire, S. Belongie, J. Hays, P. Perona, D. Ramanan, P. Dollár, and C. L. Zitnick, “Microsoft coco: Common objects in context,” in *Computer vision–ECCV 2014: 13th European conference, zurich, Switzerland, September 6–12, 2014, proceedings, part v 13*. Springer, 2014, pp. 740–755.
- [30] D. P. Kingma and J. Ba, “Adam: A method for stochastic optimization,” *arXiv preprint arXiv:1412.6980*, 2014.
- [31] G. Toderici, W. Shi, R. Timofte, L. Theis, J. Balle, E. Agustsson, N. Johnston, and F. Mentzer, “Workshop and challenge on learned image compression (clic2020),” in *CVPR*, 2020.
- [32] Z. Wang, E. P. Simoncelli, and A. C. Bovik, “Multiscale structural similarity for image quality assessment,” in *The Thirty-Seventh Asilomar Conference on Signals, Systems & Computers*, 2003, vol. 2. Ieee, 2003, pp. 1398–1402.
- [33] R. Zhang, P. Isola, A. A. Efros, E. Shechtman, and O. Wang, “The unreasonable effectiveness of deep features as a perceptual metric,” in *Proceedings of the IEEE conference on computer vision and pattern recognition*, 2018, pp. 586–595.
- [34] K. Ding, K. Ma, S. Wang, and E. P. Simoncelli, “Image quality assessment: Unifying structure and texture similarity,” *IEEE transactions on pattern analysis and machine intelligence*, vol. 44, no. 5, pp. 2567–2581, 2020.
- [35] S. Kastrulyin, J. Zakirov, D. Prokopenko, and D. V. Dylov, “Pytorch image quality: Metrics for image quality assessment,” 2022.
- [36] V. Laparra, J. Ballé, A. Berardino, and E. P. Simoncelli, “Perceptual image quality assessment using a normalized laplacian pyramid,” *Electronic Imaging*, vol. 28, pp. 1–6, 2016.
- [37] K. Ding, K. Ma, S. Wang, and E. P. Simoncelli, “Comparison of image quality models for optimization of image processing systems,” *CoRR*, vol. abs/2005.01338, 2020.
- [38] G. Bjontegaard, “Calculation of average psnr differences between rd-curves,” *ITU SG16 Doc. VCEG-M33*, 2001.